Available online at www.sciencedirect.com

ScienceDirect

Geochimica et Cosmochimica Acta 331 (2022) 35–47

Geochimica et Cosmochimica Acta

www.elsevier.com/locate/gca

Noble gas isotope systematics in the Canary Islands and implications for refractory mantle components

James M.D. Day

Scripps Institution of Oceanography, University of California San Diego, La Jolla, CA 92093-0244, USA

Received 13 May 2021; accepted in revised form 3 June 2022; available online 7 June 2022

Abstract

Noble gas isotope systematics of ocean island basalts (OIB) provide evidence for relatively undegassed and primitive mantle sources. These OIB sources partly derive from the deep mantle by virtue of their distinctiveness from mid-ocean ridge basalts (MORB), which dominantly sample upper mantle. New helium, neon and argon isotope data are presented for Canary Islands lavas, carbonatites and cumulate and mantle xenoliths confirming $^{3}He/^{4}He$ ratios that are the same or lower than MORB, but that are heterogeneous (~3–9.5R_A) within and between islands in the archipelago. Neon and Ar isotope systematics for lavas are mostly within the range of air compositions. Harzburgite xenoliths from Lanzarote, which are interpreted to represent ancient refractory mantle residues, have distinct He-Ne-Ar isotope systematics from lavas or cumulate xenoliths. The harzburgites are characterized by forsteritic olivine (>Fo_{91}) with uniformly low-$^{3}He/^{4}He$ (6.6 ± 0.2R_A), high $^{40}Ar/^{36}Ar$ (630–4900), and have Ne isotope compositions that range between air values or that are similar or more nucleogenic than depleted MORB mantle (DMM). Similar refractory mantle peridotites have been discovered as xenoliths at other OIB localities and are likely to be distinct from continental lithospheric mantle. Refractory mantle (RM), which by virtue of its high melting temperature is difficult to partially melt, may be a significant component in the convecting mantle and has potential to impart a cryptic noble gas signature to partial melts in intraplate, divergent and convergent margin settings. In this sense, RM may represent a 'sixth mantle component' after DMM, high-μ (high $^{238}U/^{204}Pb$; HIMU), enriched mantle endmembers (EMI, EMII) and the 'focus zone' (FOZO). An RM-type component may be presented in the older eastern Canary Islands and possibly in recent rejuvenated volcanism from Teide (Tenerife). Canary Island intraplate volcanism samples multiple mantle components, confirming that the most gas-rich mantle sources involved in magmatism dominate OIB noble gas compositions.

Keywords: Canary Islands; Ocean island basalt; Lavas; Xenoliths; Helium; Neon; Argon

1. INTRODUCTION

Some ocean island basalts (OIB) are considered probes into the composition of the deep mantle. From a geochemical perspective, this is primarily due to the high-$^{3}He/^{4}He$ ratios measured at some localities (e.g., Kurz et al., 1982, 2009; Hilton et al., 1999; Moreira, 2013; Marty, 2020; Day et al., 2022). Helium is a key tracer of deep mantle contributions, having a minor isotope, ^{3}He, that is primordial in origin within the Earth, and ^{4}He, which is partially primordial but also produced by radiogenic decay of U and Th. High-$^{3}He/^{4}He$ in OIB, in some cases more than twenty-five times greater than the atmospheric ratio (>25R_A; where R_A is the atmospheric ratio of $^{3}He/^{4}He$ of 1.384×10^{-6}), are considered to reflect sampling of partially degassed lower mantle distinct from the degassed upper mantle sampled by mid-ocean ridge basalts (MORB; 8 ± 2R_A; Kurz et al., 1982; Allègre et al., 1983; Kaneoka, 1983; Farley and Neroda, 1998; Graham, 2002). In particular, the locations of Loihi (Hawaii), Fernandina

E-mail address: jmdday@ucsd.edu

https://doi.org/10.1016/j.gca.2022.06.002
0016-7037/© 2022 The Author. Published by Elsevier Ltd.

(Galapagos), Ofu (Samoa), and some lavas from Iceland have been shown to have high-$^3He/^4He$, as well as similar depleted Sr-Nd-Pb isotope signatures, and so have been designated as a potential deep mantle endmember known as focus zone, or 'FOZO' lavas (e.g., Hart et al., 1992; Jackson et al., 2020).

In contrast to FOZO lavas, a significant fraction of OIB have $^3He/^4He$ ratios typically moderately above or within the range of MORB (Day et al., 2022). These include OIB that have end-member compositions reflecting extremes or mixtures of enriched mantle components. These mantle components can be recognized from high long-term time integrated Rb/Sr and low Sm/Nd suggesting derivation from evolved crustal materials (EMI, EMII), or sources with high $^{238}U/^{204}Pb$, known as HIMU (high-μ) that are considered to derive from recycled oceanic crust or lithosphere (e.g., Hofmann and White, 1982; Zindler and Hart, 1986; Hanyu and Kaneoka, 1997; Day et al., 2009, 2010). These 'extreme' compositions are found associated with FOZO lavas within islands groups such as Savaii (Samoa, EMII), Koolau, and Mauna Loa (Hawaii; EMI and HIMU), as well as in OIB without a strong FOZO signature throughout the Atlantic (e.g., Azores, Canary Islands, Cape Verde), Indian (e.g., La Réunion, Kerguelen) and Pacific Oceans (e.g., Cook-Austral Islands, French Polynesia). These OIB generally possess geochemical evidence for recycled crust and lithospheric materials in their sources based on Sr-Nd-Pb-Os isotopes (e.g., Zindler and Hart, 1986; Hofmann, 1997; Day, 2013).

Despite lack of a pronounced deep mantle signature from He isotopes, some HIMU and EM-type OIB have been shown to have a primitive 'solar' component from Ne isotopes, consistent with less degassed mantle (e.g., Staudacher et al., 1990; Poreda and Farley, 1992; Valbracht et al., 1996, 1997; Hanyu et al., 2001, 2011; Trieloff et al., 2002; Hopp and Trieloff, 2005; Madureira et al., 2005; Honda and Woodhead, 2005; Doucet et al., 2006; Parai et al., 2009; Jackson et al., 2009; Moreira et al., 2012). Neon has three stable isotopes, with ^{20}Ne and ^{22}Ne being of primordial origin, whereas ^{21}Ne is partly primordial, but also produced by (α,*n*) reactions predominantly on ^{18}O (Wetherill, 1954; Hopp and Trieloff, 2008). Consequently, radioactive decay of U and Th in Earth leads to production of nucleogenic ^{21}Ne, increasing $^{21}Ne/^{22}Ne$ over time. To date, some HIMU- and EM-type OIB have been shown to have Ne isotope compositions akin or slightly less primitive than Ne isotope compositions in FOZO OIB (e.g., Honda et al., 1993; Trieloff et al., 2000; Moreira et al., 2001; Kurz et al., 2009; Jackson et al., 2009). These data indicate that even some low-$^3He/^4He$ OIB have material sourced from relatively undegassed mantle distinct from DMM.

To describe noble gas isotope variations more fully in OIB, He-Ne-Ar isotope data are presented for Canary Island lavas and cumulate xenoliths. These samples are known to have $^3He/^4He$ generally similar to or lower than MORB (Hilton et al., 2000; Gurenko et al., 2006; Day and Hilton, 2011), and to have Sr-Nd-Os-Pb isotope signatures consistent with HIMU-type and minor EM sources (e.g., Hoernle et al., 1991; Widom et al., 1999; Gurenko et al., 2006; Day et al., 2010; Klügel et al., 2017). Additionally, He-Ne-Ar isotope data are presented for harzburgite xenoliths from Lanzarote, interpreted to reflect refractory mantle material in the oceanic lithosphere (e.g., Simon et al., 2008). Here, refractory mantle refers to peridotites that have previously experienced significant (>15%) melt depletion, and so are not expected to readily partially melt, except at high mantle potential temperatures, or if they have been metasomatized or fluxed with fluids. The Lanzarote peridotites hint at the potential for a sixth relatively cryptic 'refractory mantle' (RM) endmember after HIMU, EMI, EMII, FOZO and the depleted MORB mantle (DMM) that is not well-sampled in mantle-derived melts, but that may be important for understanding geochemical compositions of OIB, MORB and some lavas from convergent margin settings.

2. SAMPLES AND METHODS

The Canary Islands archipelago comprises seven major islands that have progressively older maximum magmatic emplacement ages from west to east (Fig. 1). Samples were selected for analysis from field campaigns in 2002, 2006 and 2009 and include shield-stage lavas from El Hierro, shield stage lavas and cumulate pyroxenite xenoliths from La Palma, a single Miocene shield stage lava and recently erupted mantle-derived harzburgite xenoliths from Lanzarote, and two approximately early Miocene aged carbonatites from Fuerteventura (Table 1). The mantle peridotites from Lanzarote were sampled at three localities and were all erupted during the 1730–1736 eruptions of Timanfaya. Mineral chemical data along with major-, trace- and stable and radiogenic data for these samples have been reported previously (Day et al., 2009, 2010; Day and Hilton 2011).

Helium trapped in fluid inclusions within optically pure olivine, pyroxene and calcite separates was released by crushing under ultra-high vacuum at the Fluid and Volatiles Laboratory, Scripps Institution of Oceanography with details of the cleaning and preparation methods outlined in Füri et al. (2010). Mineral separates were crushed *in vacuo*, releasing volatiles trapped as fluid inclusions and avoiding cosmogenic or radiogenic components (e.g., Hilton et al., 1993). Helium was expanded into a stainless-steel preparation line and sequentially exposed for a total of 30 minutes to a Ti getter at 750°C, decreasing to 400°C, followed by a liquid N-cooled charcoal trap, a SAES© Zr-Al getter operated at room temperature, and a He-cooled charcoal trap, to isolate helium from neon. Purified helium was expanded into a dual-collector noble-gas mass spectrometer (MAP 215E) for $^3He/^4He$ analysis using a peak-jumping protocol (Shaw et al., 2001). Raw helium-isotope ratios were normalized using standard aliquots of SIO Pier air (1 R_A), under the same preparation and measurement procedures used for samples. Neon was monitored during each run, to correct $^3He/^4He$ and He concentrations for potential air-contamination.

Neon and Ar abundances and isotope ratio determinations were performed on a subset of samples. Optically pure olivine and pyroxene separates were loaded into screw-type crushers that were evacuated to ultrahigh vacuum and kept

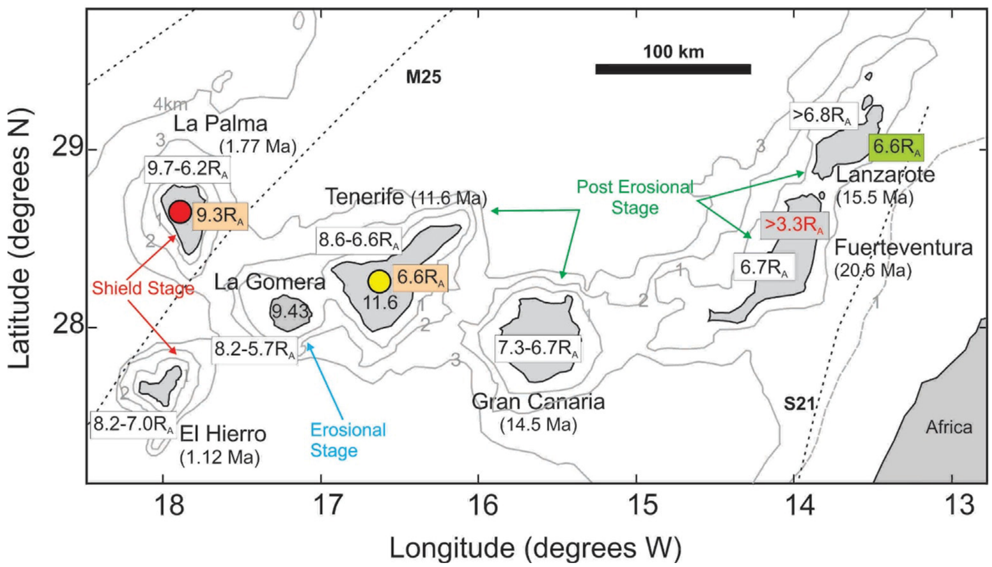

Fig. 1. Map of the Canary Islands with helium isotope data from olivine and pyroxene separates from lavas and cumulate xenoliths, for carbonatites from Fuerteventura in the grey filled box with red letters, and mantle harzburgite xenoliths from Lanzarote in the green box. Geothermal fluids and gas sample compositions from Teide (yellow circle) and Taburiente (red circle) are also shown (from Day and Hilton, 2021). Maximum and minimum He isotope compositions (as $^{3}He/^{4}He$ [R_A]) measured in olivine are given in the boxes for each island and are from Gurenko et al. (2006), Day and Hilton (2011), Carnevale et al. (2021), and this study. Oldest erupted lava ages are given in parentheses after the island name in millions of years, or within the island boundaries and are summarized in Day et al. (2010). Current growth stages of the Canary Islands are shown as are ocean floor depths (km) and palaeomagnetic anomalies M25 and S21. S21 lies close to the juncture of the continental/oceanic lithosphere boundary.

at 100°C overnight. Neon and Ar abundances and isotope ratios of $^{22}Ne/^{20}Ne$, $^{21}Ne/^{20}Ne$ and $^{40}Ar/^{36}Ar$ were determined on a modified VG5400 mass spectrometer equipped with five Faraday cups and a Daly photo-multiplier detector in peak jumping mode (see Craig et al., 1993; Füri et al., 2010). Gases were released from samples by single step crushing in vacuo using an external five-ton hydraulic press. After removal of other volatile species, Ne was released from a cryogenic trap at 90 K. Reproducibility of Ne isotope analyses was monitored using an air standard measured after every eight sample runs or fewer, and sample Ne isotope compositions were determined by normalization to an air standard. Neon results were corrected for procedural blanks and contributions of double-charged ^{40}Ar and CO_2 to ^{20}Ne and ^{22}Ne, respectively, following Niedermann et al. (1993), with the explicit method used here discussed in Füri et al. (2010). Procedural blanks were run prior to each individual sample averaged 0.5×10^{-9} cm^3 ^{4}He, 0.002×10^{-9} cm^3 ^{20}Ne, and 6×10^{-9} cm^3 ^{40}Ar. These blanks result in blank corrections of less than 10% of sample yields in most cases for He and <2% for Ne and Ar. Exceptions were the LZ0601 pyroxene separate and LZ0604 olivine for He. Higher blank contributions are typically due to low intrinsic gas contents and/or restricted available masses for some samples (Table 1).

3. RESULTS

New He, Ne and Ar isotope results are presented in Table 1, with full abundances and ratios presented in Table S1. These data complement and extend previously published data for the Canary Islands (Vance et al., 1989; Perez et al., 1994; Hilton et al., 2000; Gurenko et al., 2006; Day and Hilton, 2011, 2021; Grachev, 2012; Carnevale et al., 2021) demonstrating heterogenous distribution of helium isotopes across the archipelago and within islands (Fig. 1). The new He isotope and abundance data for El Hierro (7.2–8.2R_A) and La Palma (7.5–7.6R_A) are within the range of previously reported data, with the new La Palma helium isotope data derived exclusively from pyroxenite xenoliths. A single Miocene Lanzarote ankaramite was measured, with the olivine having higher $^{3}He/^{4}He$ (6.9R_A) and He content than the corresponding clinopyroxene (3.2R_A) (Fig. 2). Nine harzburgite samples were measured from three distinct locations on Lanzarote, yielding homogeneous $^{3}He/^{4}He$ (6.6 ± 0.2R_A; 2 St. Dev) and generally high He gas contents (3 to 314 × 10^{-9} cm^3 g^{-1}). Calcite grains from two Miocene carbonatites on Fuerteventura were analyzed, giving low $^{3}He/^{4}He$ (2.6–3.3R_A) and high gas contents (205 to 2050 × 10^{-9} cm^3 g^{-1}).

Six El Hierro lavas were measured for neon and argon isotopes, defining a range in $^{20}Ne/^{22}Ne$ from 9.71 to 9.96 and $^{21}Ne/^{22}Ne$ from 0.0289 to 0.0294 that are identical, within uncertainties, to air. These samples have $^{40}Ar/^{36}Ar$ identical (296) to discernable (414) from air, with the highest Ne and Ar contents in the single pyroxene separate that was analyzed (Fig. 3). Neon and Ar isotope analyses were conducted for five La Palma lavas and cumulate xenoliths, revealing a similar range in Ne isotopic compositions ($^{20}Ne/^{22}Ne$ = 9.67–9.94; $^{21}Ne/^{22}Ne$ = 0.0291–0.0293) to El Hierro, with all having $^{40}Ar/^{36}Ar$ analytically

Table 1
Helium, neon and argon isotope systematics of Canary Island volcanic rocks and xenoliths.

Sample	Location	Age (Ka)	Lat (N) DTM	Long (W) DTM	Rock Type	Mineral	Fo	±2σ	Mass He (g)	R/R$_A^b$	X^c	R$_C$/R$_A$	±2σ	^{4}He (10^{-9} cm^3 g^{-1})	Blank %	Mass Ne-Ar (g)	^{20}Ne/^{22}Ne	±2σ	^{21}Ne/^{22}Ne	±2σ	^{20}Ne (10^{-9} cm^3 g^{-1})	Blank %	^{40}Ar/^{36}Ar	±2σ	^{40}Ar (10^{-9} cm^3 g^{-1})	Blank %
El Hierro																										
EH0601	Lomo Negro	<10	274522	180853	Ankaramite	Ol	84.0	3.4	1.29	7.72	445	7.74	0.08	48.9	2%	3.02	9.79	0.05	0.0287	0.0002	0.166	0.4%	313	6	146	1.3%
EH0602	Faro De Orchilla	<1	274227	180849	Ankaramite	Ol			1.20	7.85	181	7.88	0.08	32.3	3%											
EH0603	Tamaguste	<10	274747	175516	Alkali Basalt	Ol			0.84	8.22	812	8.23	0.07	115	1%											
EH0604	Pozo De La Salud	<10	274525	180611	Basanite	Ol			1.12	7.90	2004	7.90	0.08	34.8	2%	2.11	9.71	0.05	0.0292	0.0002	0.058	1.6%	414	8	53	5.1%
JMDD EH01	Faro De Orchilla	<1	274522	180854	Ankaramite	Ol	81.5	5.6	1.25	7.79	640	7.80	0.10	47.9	2%											
						Cpx	76.4	3.6	1.45	7.79	32	8.01	0.14	15.9	4%											
JMDD EH10	Ermita de la Virgen	160	274758	175850	Ankaramite	Ol^a	78.3	0.6				*7.52*	*0.45*	*3.6*		3.21	9.83	0.05	0.0289	0.0002	0.322	0.2%	307	6	335	0.56%
JMDD EH13	Ermita de la Virgen	135	274805	175848	Ankaramite	Ol^a	79.4	3.6				*8.17*	*0.31*	*13.3*		2.03	9.76	0.05	0.0294	0.0002	0.087	1.1%	394	8	159	1.82%
						Cpx^a	77.4	6.4				*4.15*	*0.14*	*18.2*		2.37	9.96	0.05	0.0291	0.0002	2.851	0.03%	296	6	2628	0.10%
JMDD EH15	Ermita de la Virgen	335	274739	175901	Ankaramite	Ol^a	81.7	4.5				*7.81*	*0.29*	*10.5*		1.99	9.87	0.05	0.0291	0.0002	0.522	0.2%	300	6	342	0.87%
La Palma																										
LP0601	Tazacorte	100	283837	175630	Clinopyroxenite	Cpx			1.20	7.45	40	7.61	0.08	40.9	2.0%	2.09	9.82	0.05	0.0293	0.0002	1.341	0.1%	328	7	477	0.60%
LP0602A	San Antonio	3	282859	175105	Clinopyroxenite	Cpx			1.04	7.11	20	7.43	0.14	24.7	3.7%											
						Cpx			0.98	7.5	306	7.53	0.09	554	0.2%	0.98	9.93	0.05	0.0293	0.0002	3.204	0.1%	504	10	1115	0.55%
LP0603	Fuente Santa	3	282737	175057	Ol Clinopyrox.	Ol	90.3	0.2	1.03	7.46	738	7.47	0.07	57.0	1.7%											
JMDDLP01	Garafia	1440	284546	174918	Ankaramite	Ol^a	81.4	3.0				*7.2*	*0.4*	*4.6*		1.87	9.93	0.09	0.0291	0.0004	0.036	2.9%	336	6	174	1.8%
JMDDLP02	Garafia	1440	284552	174904	Ankaramite	Ol^a						*7.5*	*0.2*	*38.4*		2.01	9.84	0.10	0.0292	0.0003	0.021	4.6%	429	8	171	1.7%
JMDDLP03	Pliocene Seamount	3000	284048	175502	Picrite	Ol^a	83.3	1.6				*9.7*	*0.3*	*1.9*		2.57					0.007	10.0%	354	7	167	1.4%
JMDDLP05	Taburiente	1020	284615	175153	Ankaramite	Cpx^a						*6.8*	*0.2*	*37.1*		2.88	9.67	0.12	0.0292	0.0002	0.048	1.4%	437	8	61	3.3%
Lanzarote																										
LZ0601	Salinas Del Janubio	~12000	285621	134904	Ankaramite	Ol	84.8	0.3	1.02	6.85	−999	6.85	0.09	21.7	4%	2.06	9.85	0.05	0.0322	0.0003	0.032	2.9%	502	10	232	1.2%
						Cpx			1.56	3.16	54	3.20	0.10	2.4	21%											
LZ0602a	De Los Cuervos	<0.1	285951	134152	Harzburgite	Ol	91.3	0.2	3.22	6.54	217	6.56	0.07	11.2	3%	2.97	10.00	0.05	0.0296	0.0002	0.277	0.2%	2039	41	790	0.25%
LZ0602b	De Los Cuervos	<0.1	285,951	134,152	Harzburgite	Ol	91.4	0.2	3.25	6.66	255	6.68	0.07	16.2	2%	3.13	9.82	0.05	0.0288	0.0002	0.197	0.3%	1668	33	666	0.29%
LZ0603	De Los Cuervos	<0.1	285951	134152	Harzburgite	Ol	91.7	0.3	3.25	6.5	551	6.50	0.20	10.7	3%	3.09	9.91	0.05	0.0298	0.0002	0.346	0.2%	1875	38	913	0.21%
LZ0604	Pico Partido	<0.1	290037	134309	Harzburgite	Ol			1.00	6.29	25	6.52	0.22	3.3	23%	2.02	9.79	0.05	0.0294	0.0002	0.109	0.9%	634	13	149	1.95%
LZ0604a	Pico Partido	<0.1	290037	134309	Harzburgite	Ol	91.3	0.6	3.28	6.56	1123	6.56	0.05	28.2	1.1%	3.77	9.86	0.05	0.0308	0.0002	0.065	0.8%	1407	28	219	0.72%
LZ0604b	Pico Partido	<0.1	290037	134309	Harzburgite	Ol	91.7	0.4	2.58	6.53	443	6.54	0.07	20.1	1.9%	3.14	9.83	0.05	0.0300	0.0002	0.051	1.2%	2187	44	361	0.53%
LZ0604c	Pico Partido	<0.1	290037	134309	Harzburgite	Ol	91.6	0.3	2.03	6.69	2346	6.69	0.05	314	0.2%	3.05	9.98	0.05	0.0312	0.0002	0.307	0.2%	4896	98	2697	0.07%
LZ0604d	Pico Partido	<0.1	290037	134309	Harzburgite	Ol	91.4	0.1	3.17	6.7	2727	6.70	0.05	47.4	0.7%	3.32	9.89	0.05	0.0300	0.0002	0.082	0.7%	1845	37	430	0.42%
LZ0605	Montana De La Nuces	<0.1	290037	134309	Harzburgite	Ol	91.2	0.1	3.07	6.64	1453	6.60	0.10	48.1	0.7%	3.25	10.32	0.05	0.0336	0.0003	0.137	0.4%	4923	98	1983	0.09%
Fuerteventura																										
FE 0602	Ajuy	~20000	282354	140968	Carbonatite	CC			1.15	3.27	3099	3.27	0.10	2030	0.04%											
FE 0606	Fuerteventura	~20000	282352	140969	Carbonatite	CC			0.37	2.64	825	2.64	0.09	205	1.3%											

Latitudes and londitudes are given in Universal Transverse Mercator. Mineral abbreviations are: Ol = olivine; Cpx = clinopyroxene; CC = calcite. Ages are in Ka and are from sources in Day et al. (2010) or Carracedo and Troll (2016). Lanzarote harzburgites were all emplaced during the Timanfaya eruptive event.

a: Helium isotope analyses from Day and Hilton (2011). Olivine forsterite (Fo) contents (Mg/[Mg + Fe] × 100 in atomic formula units) are from the same work.

b: R/R$_A$ notation where R = sample ^{3}He/^{4}He ratio and R$_A$ = atmosphere ^{3}He/^{4}He ratio (=1.38 × 10^{-6}).

c: X = (^{4}He/^{20}Ne)$_M$/(^{4}He/^{20}Ne)$_{air}$, where $_M$ refers to the measured ^{4}He/^{20}Ne ratio. R$_C$/R$_A$ is the air-corrected He isotope ratio = [(R/R$_A$ × X) − 1]/(X − 1). Note that X values are not reported for the previously published He isotope data.

All He, Ne and Ar data are blank corrected with blank contributions as percentages of total gas samples shown.

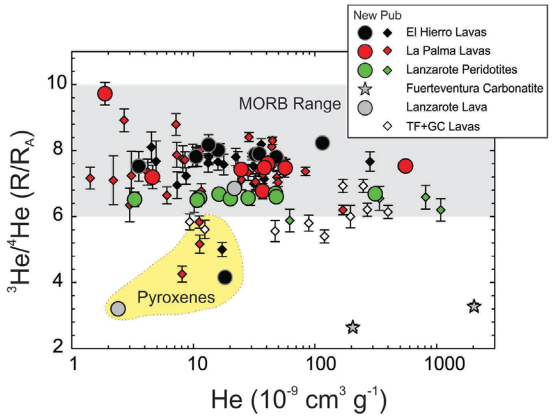

Fig. 2. Compilation of helium isotope and He abundance data for lavas and xenoliths from the Canary Islands. Shown is the typically accepted MORB range of $8 \pm 2R_A$ from Graham (2002) and the field of pyroxene compositions from ankaramites on El Hierro, La Palma and Lanzarote. Data are from this study (New symbols), Vance et al. (1989), Hilton et al. (2000), Day and Hilton (2011) and Grachev (2012) (Pub[lished] symbols in the key).

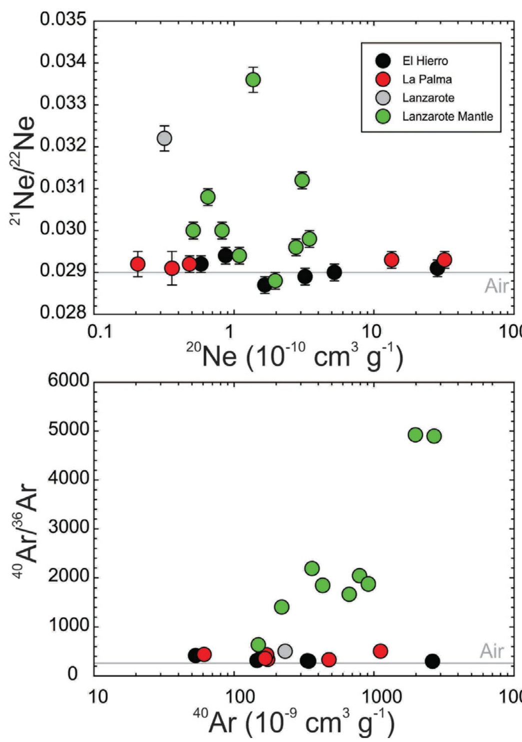

Fig. 3. Neon and argon isotope and abundance systematics for lavas and xenoliths (Lanzarote mantle) from the Canary Islands analyzed in this study. Shown are the $^{21}Ne/^{22}Ne$ and $^{40}Ar/^{36}Ar$ ratios for air for comparison.

distinguishable from air (328–504). Olivine from the Lanzarote ankaramite had a non-air Ar isotope composition (502), and low $^{20}Ne/^{22}Ne$ (9.85) and high $^{21}Ne/^{22}Ne$ (0.0322). Lanzarote harzburgites have elevated Ne and Ar gas contents, high $^{40}Ar/^{36}Ar$ (634–4923) and $^{20}Ne/^{22}Ne$ ranging from 9.82 to 10.32 and $^{21}Ne/^{22}Ne$ from 0.0258 to 0.0336 (Fig. 4).

Neon isotope data should only be discussed in the context of mantle sources if they are statistically outside of analytical uncertainties of the air value. For the data presented here, the generally low $^{20}Ne/^{22}Ne$ (typically < 10.3), and air-like $^{21}Ne/^{22}Ne$ of most samples precludes them from further discussion of mantle components. Only the LZ0605 harzburgite olivine has $^{20}Ne/^{22}Ne$ and $^{21}Ne/^{22}Ne$ > 2 standard deviations above the air ratio within the dataset (Fig. 4). Extrapolations to a presumed $^{21}Ne/^{22}Ne$ composition assuming a $^{20}Ne/^{22}Ne$ of 12.5 gives a value for this sample of 0.0529 ± 0.0047.

4. DISCUSSION

4.1. Helium isotopes variations in the Canary Islands and in carbonatites

New helium isotope data for Canary Island samples confirms relative homogeneity in $^3He/^4He$ for La Palma and El Hierro and expands the range of He isotope variations measured in the Canary Islands. The new data support previous observations of disequilibrium in He isotope compositions between some – but not all - olivine and pyroxene separates in Canary Island lavas (Hilton et al., 2000; Day and Hilton, 2011). These differences have been attributed to modification through ingrowth of ^4He during Th and U decay within pyroxene grains, as well as through degassing and assimilation, with limited evidence for other possible post-crystallization processes. Typically, pyroxenes with relatively low He gas contents are most susceptible to ingrowth of ^4He, and this is well-demonstrated for the mid-Miocene Lanzarote ankaramite which has olivine with $^3He/^4He$ of $6.9R_A$, but pyroxene with a relatively low gas content and low-$^3He/^4He$ (Fig. 2). Previous quantitative aging models from Day and Hilton (2011) are consistent with the low-$^3He/^4He$ pyroxene separates resulting from degassing and aging processes, such that these data are not considered further in the He isotope variations for the Canary Islands (Fig. 1). Lava and cumulate xenolith olivine and geothermal fluid and gas compositions confirm limited ($\sim 5R_A$ total variation) but heterogeneous variations in $^3He/^4He$ that occur within and between the islands in space and time (e.g., Day and Hilton, 2021). The overall relationship is for higher $^3He/^4He$ in the main shield building phase of volcanism of the western Canary Islands compared to the easternmost islands in the archipelago.

As shown previously (Day and Hilton, 2011), there are no observable correlations between He isotopes and olivine composition in Canary Island lavas (Fig. 5). El Hierro olivine grains have generally constant $^3He/^4He$ for a range of forsterite contents, whereas La Palma olivine compositions are more variable but lie within a similar field of forsterite compositions. The lavas have olivine that are distinct from the Lanzarote harzburgite xenoliths which have higher forsterite contents (>91) and lower $^3He/^4He$ ($\sim 6.6R_A$). The harzburgite xenoliths have similar helium isotope compositions but higher forsterite contents compared with what are interpreted as recent mantle lithosphere from beneath the

West Antarctic Rift (Day et al., 2019). These compositions are likely to be similar to those estimated for subducted oceanic lithosphere (Moreira and Kurz, 2001). Conversely, Lanzarote xenoliths have lower forsterite contents but higher $^3He/^4He$ than relatively recently erupted continental lithospheric mantle peridotites (Fig. 5).

Two Fuerteventura carbonatite samples were measured for He isotope compositions in calcite separates, with every attempt to avoid addition of apatite or other high U + Th phases, and these separates gave high He gas contents and low $^3He/^4He$ (2.6–3.3R_A). These data compliment a study of He-Ne-Ar isotopes in apatite (0.003–0.08R_A), calcite (3.4–3.9R_A) and pyroxene (2.2R_A) from Fuerteventura carbonatite, illustrating the radiogenic He present in apatite grains (Carnevale et al., 2021). The Fuerteventura carbonatites represent only the second occurrence of OIB carbonatites studied for He isotope compositions. The best studied OIB carbonatites are those from Cape Verde, where Mata et al. (2010) showed that apatite grains generally recorded more radiogenic He isotope compositions (0.03–9.8R_A) than calcite grains (6.7–15.5R_A) due to high U and Th and potential for ^4He in growth in the former. The Fuerteventura carbonatites are older (~15 Ma or more) than those from Cape Verde (~2–9 Ma) and have been dissected by dikes and later intrusions, with recrystallization of calcite along cross-cutting contacts. It is probable, therefore, that the He isotope compositions of Fuerteventura carbonatites provide a minimum $^3He/^4He$ for their parental melts after post-crystallization modification. This argument would be consistent with the higher reported He isotope composition for a clinopyroxenite from Fuerteventura (6.7R_A; Carnevale et al., 2021).

4.2. Neon isotope composition of Canary Islands volcanism

Entrainment of air within lavas and magmas is a chronic issue in the study of heavier noble gases (Ne, Ar, Kr, Xe) in OIB (e.g., Farley and Neroda, 1998). For example, geothermal fluids and gases from Teide (Tenerife) and Taburiente (La Palma) have Ne isotope compositions compromised by air entrainment (Day and Hilton, 2021). An important distinction between geothermal samples and olivine and pyroxene grains from melts is that the potential mechanisms for contamination are distinct. Mineral separate analyses properly corrected for analytical blank contributions to express the Ne isotope composition are most likely to reflect any air entrainment coming from assimilation into parental melts. In some cases, it is also possible that smaller grain size samples crushed for noble gas analyses may also retain higher atmospheric noble gas contents on their surfaces (selected grains measured here were >0.5 mm or greater in average diameter). Such processes are known to occur in OIB and have the potential to overwhelm mantle source compositions (Farley and Neroda, 1998; Moreira, 2013). Indeed, despite limited total measurements, low measured $^{20}Ne/^{22}Ne$ have been reported previously for HIMU-type OIB localities (e.g., Hanyu et al., 2011).

Mineral separates from La Palma and El Hierro lavas and cumulate xenoliths have neon isotope compositions that are limited and lie within the range of air-like Ne (Figs. 3 and 4), but with $^{40}Ar/^{36}Ar$ distinct from air (Fig. 6). It has been shown that some OIB have neon isotope compositions that form correlations in $^{20}Ne/^{22}Ne$-$^{21}Ne/^{22}Ne$ space only slightly more nucleogenic than the solar composition. These locations include Loihi, Iceland, and Fernandina in the Galapagos Islands (Valbracht et al., 1997; Trieloff et al., 2000; Moreira et al., 2001; Kurz et al., 2009; Füri et al., 2010; Mukhopadhyay, 2012; Péron et al., 2017). Solar Ne components have also been observed in Ofu (Samoa; Jackson et al., 2009), Terceira (Azores; Madureira et al., 2005), and even the EMI end-member, Pitcairn (Honda and Woodhead, 2005). Other locations have MORB-like Ne isotope compositions, as observed in the Cook-Austral Islands (Parai et al., 2009; Hanyu et al., 2011). Due to the limited range in Ne isotope compositions that are within uncertainty of air, the new results for Canary Islands lavas do not define a distinct end-member in Ne isotope space. Analytical improvements and careful selection of samples are likely to enable improvement upon this result in the future.

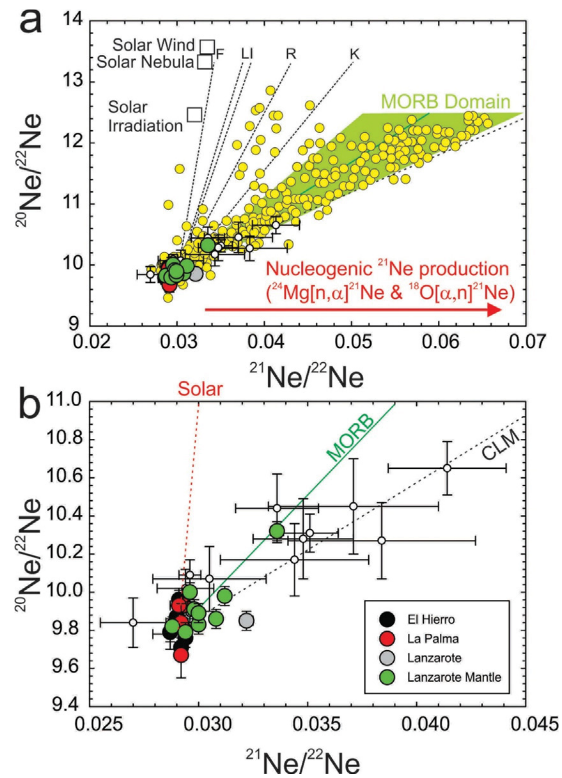

Fig. 4. (a) Three-neon isotope plot for lavas and xenoliths from the Canary Islands compared with mid-ocean ridge basalts (yellow circles), European continental lithospheric mantle (CLM) peridotites (unfilled circles), and compositions of putative solar components (unfilled squares). (b) Neon three-isotope diagram for lavas and xenoliths from the Canary Islands with the solar (Black, 1972; Benkert et al., 1993), MORB (Sarda et al., 1988) and CLM Ne isotope correlations shown for comparison. Data for MORB are from Moreira (2013) and references therein, with the examples from the European CLM from Gautheron et al. (2005). F = Fernandina; L = Loihi; I = Iceland; R = La Réunion; K = Kerguelen.

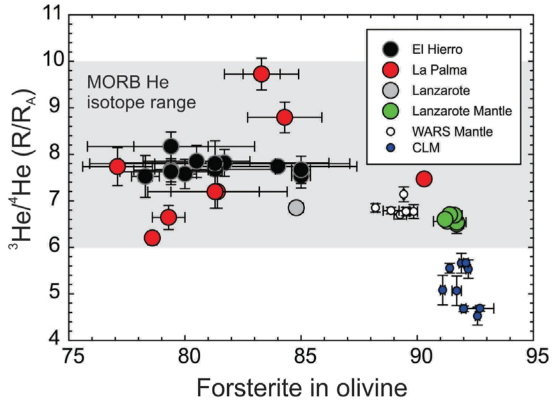

Fig. 5. Helium isotope composition versus the forsterite content (molar Mg/[Mg + Fe] × 100) in olivine for samples analyzed in this study. Shown is the typically accepted MORB range of 8 ± 2R_A from Graham (2002) and the compositions of West Antarctic Rift System (WARS) peridotites from Day et al. (2019) and for continental lithospheric mantle xenoliths erupted within <100-million-year-old kimberlites from Day et al. (2015).

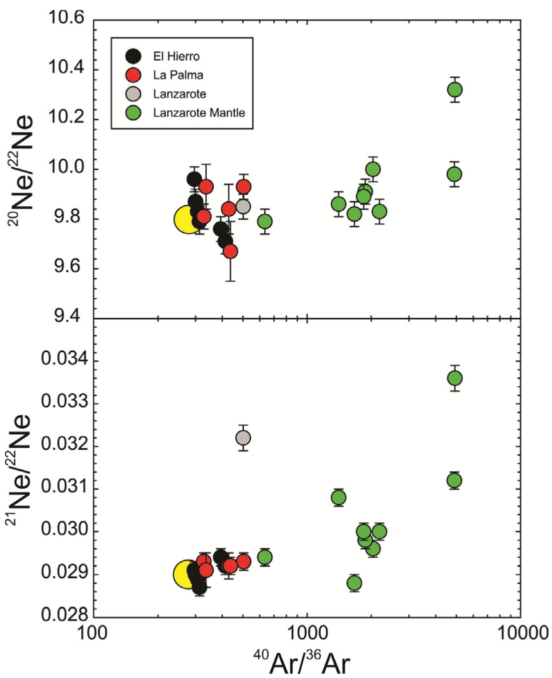

Fig. 6. Neon-argon isotope systematics for Canary Island lavas and xenoliths. The yellow circle denotes the Ne-Ar isotope compositions for air ($^{20}Ne/^{22}Ne$ = 9.8; $^{21}Ne/^{22}Ne$ = 0.029; $^{40}Ar/^{36}Ar$ = 298.6).

4.3. The plausibility of nucleogenic neon in ancient, refractory low-$^3He/^4He$ mantle

In contrast to the limited Ne isotope variations in Canary Island lavas and cumulate xenoliths, harzburgite xenoliths from Lanzarote are distinct with low $^{21}Ne/^{22}Ne$ for a given $^{20}Ne/^{22}Ne$ ratio (Fig. 4), with LZ0605 having $^{20}Ne/^{22}Ne$ > 10.3. The harzburgites are strongly melt-depleted rocks containing only olivine, orthopyroxene and spinel as major phases. They can be interpreted as fragments of refractory mantle based on textures, olivine compositions (>Fo_{91}), bulk rock compositions and Os isotope systematics that suggest melt depletion ages of >500 Ma in some instances (e.g., Widom et al., 1999; Simon et al., 2008; Grachev, 2012). These characteristics make the Lanzarote harzburgites similar to peridotites from other ocean islands (e.g., Simon et al., 2008; Snortum et al., 2019), with depletion ages similar to or older than those measured in abyssal peridotites (Day et al., 2017), suggestive of their inclusion within the oceanic mantle. An alternative possibility is that the Lanzarote harzburgites represent continental lithospheric mantle isolated during opening of the North Atlantic. The harzburgite xenoliths have remarkably consistent helium isotope compositions (6.6R_A), akin to calculated compositions of oceanic lithosphere (Moreira and Kurz, 2001), as well as to recently formed mantle lithosphere (Day et al., 2019). Given that these xenoliths contain spinel and have equilibration temperatures consistent with a shallow origin (Simon et al., 2008), they can also be interpreted as now forming part of the Atlantic oceanic lithosphere that the Canary Islands are built upon.

Despite the refractory nature of the Lanzarote peridotites, from a noble gas perspective, xenoliths can be susceptible to open-system behavior from cryptic metasomatic effects and melt infiltration (e.g., Burnard et al., 1998; Day et al., 2015). Gas release experiments on a single OIB-entrained xenolith have shown that such rocks can record complex histories that include diffusion and incorporation of noble gases (Burnard et al., 1998). Single crush experiments, like those employed here, may therefore release more than a single generation of gas from the separated olivine. In the field, there is evidence for melt infiltration in some Lanzarote peridotite xenoliths in the guise of melt-veins and darkened patches with pervasive melt infiltration. Samples without these characteristics were selected for this study. Nonetheless, the single crush experiments could reflect interaction with the xenoliths and mantle-derived melts, especially during recent volcanic activity at Lanzarote. Alternatively, the xenoliths are unaffected by such processes and accurately record a source composition linked to their prior melt depletion. As argued below, in either case, He-Ne-Ar isotope systematics of the Lanzarote peridotites suggest derivation from a relatively refractory reservoir.

The harzburgite xenoliths have Ne isotope compositions that suggest a composition similar to, or more radiogenic than, MORB. As noted previously, all Ne isotope variations in terrestrial rocks that exclude atmospheric contributions reflect mixtures between primordial contributions ($^{20,21,22}Ne$) and ^{21}Ne that is produced dominantly by α, *n* reactions on ^{18}O (Wetherill, 1954). Differences between OIB with primitive components and with MORB reflect greater degassing in the source of the latter, with corresponding decay of radioactive nuclides (U, Th) that engender nucleogenic Ne formation, especially in ultramafic rocks. For these reasons, nucleogenic Ne occurs in the depleted mantle source of MORB as well as in continental lithospheric mantle peridotites (e.g., Hopp et al., 2004, 2007; Gautheron et al., 2005; Buikin et al., 2005) (Fig. 4). Noble gas compositions of Lanzarote harzburgite xenoliths can be interpreted to reflect an equal or greater degree of noble gas loss than in the MORB mantle source, coupled with radiogenic ingrowth of ^{4}He and generation of nucleogenic ^{21}Ne in the source. The most likely mode for gas loss (degassing) is through melt depletion processes acting to form refractory lithosphere. In addition to degassing, melt depletion in peridotites will deplete incompatible radiogenic elements, including K, Th and U. Consequently, nucleogenic ingrowth of ^{21}Ne and branch-decay of ^{40}K to ^{40}Ar in melt-depleted peridotites will be reduced. A feature of ancient, refractory mantle will therefore be for more nucleogenic neon compared with DMM and relatively low-^{3}He/^{4}He that is distinct from K, U and Th-rich crustal rocks which will trend to strongly nucleogenic Ne and low ^{3}He/^{4}He (<$1R_A$) with time (e.g., Day et al., 2015).

To calculate likely evolution characteristics of refractory mantle, ingrowth for He isotopes can be calculated assuming that melt depletion is the cause of the variations at ~500 million years ago based on Os isotope model ages for Lanzarote peridotites (Simon et al., 2008). Assuming refractory mantle U and Th contents (e.g., Day et al., 2015), a MORB ^{3}He/^{4}He initial composition and He contents within the range of lithospheric mantle sources (e.g., Moreira and Kurz, 2001) will result in a ^{3}He/^{4}He of ~$6R_A$, slightly lower than the measured values. Since, under these conditions, He and Ne are coupled with a ^{21}Ne/^{4}He production ratio of ~4.5×10^{-8} (Yatsevich and Honda, 1997), the ^{21}Ne/^{22}Ne can also be predicted to evolve to nucleogenic compositions with time, as observed in the samples. Refractory mantle, unaffected by later melt refertilization or metasomatism, should have lower ^{3}He/^{4}He than DMM, develop nucleogenic Ne with ^{20}Ne/^{22}Ne at or below MORB values and, depending on formation age, have lower ^{40}Ar/^{36}Ar than MORB, due to long term removal of K, regardless of location. As noted previously, refractory mantle is not uncommon in the convecting mantle; similar materials to those found in Lanzarote also occur in all ocean basins, evident from the refractory compositions and ancient osmium isotope model ages for OIB xenolith suites (e.g., Simon et al., 2008; Snortum et al., 2019).

4.4. Signatures of refractory mantle sources in mantle-derived melts?

Helium-Ne-Ar isotope compositions of Lanzarote harzburgite xenoliths are relevant to the Canary Islands and may have wider implications for global refractory mantle reservoirs. In the case of the Canary Islands, the distinctive isotopic compositions of the harzburgite xenoliths emphasize that mantle sources to recent lavas from El Hierro and La Palma are separate from this reservoir, indicating that refractory mantle has no obvious role in the generation of their parental melts, and consistent with their enriched trace element character (e.g., Hoernle et al., 1991; Gurenko et al., 2006; Day et al., 2010). Conversely, the He-Ne isotope composition of the Lanzarote ankaramite (LZ0601) could be considered broadly akin to the harzburgites. This ankaramite is from the main shield phase of volcanism, raising the possibility that there may have been a greater refractory mantle contribution earlier in the history of Canary Islands magmatism. Fuerteventura carbonatites appear to have a distinct Ne isotope composition (Carnevale et al., 2021) to Lanzarote harzburgites, suggesting that they also have a distinct non-lithospheric source, possibly through recycling of surface carbonate material (e.g., Amsellem et al., 2020).

In addition to possible evidence for lithospheric mantle sources in eastern Canary Island lavas, there is similarity in He isotope compositions measured for geothermal gas samples on the summit of Teide versus the Lanzarote harzburgite xenoliths (Fig. 1). This is particularly notable as lavas from the main shield phase of Tenerife had higher ^{3}He/^{4}He than the present-day gas samples from Teide (Day and Hilton, 2021). A possible cause of variability is that the current magmatism beneath Teide receives gases dominantly from a refractory lithospheric mantle component beneath the island. Differences in source between shield stage and later volcanism could potentially explain the heterogeneous distribution of helium isotopes observed in the Canary Islands. Earlier volcanism in the eastern Canary Islands, and later rejuvenated volcanism, both in Teide but also in Gran Canaria likely tap mantle sources with a refractory mantle noble gas composition. A refractory mantle composition may also be consistent with models for heterogeneous sources based on Sr-Nd-Pb isotopes (Hoernle et al., 1991) if this component could be linked to an enriched mantle signature for lithophile isotopes. Such a scenario could arise if melt refertilization processes act to modify and overprint incompatible trace elements in refractory mantle reservoirs.

Rejuvenated volcanism in some Pacific OIB has been interpreted to reflect partial melting of otherwise depleted lithospheric mantle sources that have been metasomatized or melt infiltrated, likely during passage over the hotspot responsible for main shield volcanism (e.g., Bianco et al., 2005; Paquet et al., 2019). As shown with the Lanzarote harzburgite xenoliths, strongly melt depleted mantle should have ^{3}He/^{4}He and ^{21}Ne/^{22}Ne lower than MORB. However, rejuvenated partial melts from lithospheric melting might be expected to be a mixture of such sources as well as from metasomatizing melts and fluids. For example, Juan Fernandez rejuvenated lavas have He-Os isotope systematics interpreted to reflect addition from underlying hotspot metasomatism (Paquet et al., 2019). In the Hawaiian arch, where alkalic lavas have a lithospheric flexure origin but have not gone over the plume, they have MORB-like He and Ne ratios (Hanyu et al., 2005). These relationships suggest that depleted or refractory mantle sources are relatively easily overwhelmed by asthenospheric mantle melt sources due to higher noble gas contents in the latter. The effect of melt depletion followed by metasomatism by hotspot melts can potentially explain the noble gas systematics of harzburgite xenoliths from the rejuvenated stage of Savai'i (Samoa) which have elevated ^{3}He/^{4}He ($11R_A$), but also have more nucleogenic Ne and lower He isotope ratios than peridotite xenoliths closer to the hotspot center (Poreda and Farley, 1992). Strongly melt-depleted and refractory mantle sources that are subsequently metasomatized may only be expected to leave a cryptic noble gas imprint on rejuvenated sources.

Partial melting of refractory mantle with or without melt refertilization might also explain the variability in noble gas compositions measured in some MORB (e.g., Parai et al., 2012; Tucker et al., 2012), as well as in settings around subduction zones (Shaw et al., 2001). It has been proposed, based on lithophile element systematics, that components of the convecting mantle are more depleted than DMM (e.g., Stracke et al., 2011). Geodynamic models of mantle convection imply a significant fraction of the mantle has been melt depleted through time (Day et al., 2022). If such reservoirs are isolated for long-time periods, they could develop noble gas compositions akin to those in Lanzarote harzburgite xenoliths, and so the noble gases may be useful for revealing such a source. Shaw et al. (2001) reported decoupling of He from Ne isotopes, and the presence of a nucleogenic component in Manus Basin back arc basalts. They interpreted these compositions to reflect either deep mantle source heterogeneity or a degassing event leaving a Ne-depleted reservoir. The presence of a high-^{3}He/^{4}He hotspot component interacting with refractory mantle would potentially be consistent with the Manus Basin data. Refractory mantle noble gas signatures may be cryptically preserved in both divergent and convergent margin settings suggesting that refractory or ultra-depleted mantle domains are widespread (e.g., Stracke et al., 2019; Day et al., 2022). Refractory mantle formed within the convecting mantle versus from erosion of continental lithospheric mantle may be difficult to distinguish, unless the latter was strongly affected by metasomatism, or more strongly melt depleted. A potential argument against significant continental lithospheric mantle material within the oceanic mantle is also the widespread existence of refractory peridotites found in ocean islands (e.g., Simon et al., 2008), which would require extensive prior destruction of continental lithosphere. Further work is needed to determine between these possibilities and the role that refractory mantle might play in the generation of partial melts at Earth's surface.

4.5. Implications for noble gas and radiogenic isotope systematics in ocean islands

A geochemical observation for some OIB is that they must be partly sourced from the deep mantle due to the presence of high-^{3}He/^{4}He in localities such as Iceland, Samoa (Ofu), Galapagos (Fernandina) or Hawaii (Loihi) (e.g., Kurz et al., 1982, 2009; Honda et al 1993; Hilton et al., 1999; Graham, 2002; Jackson et al., 2009). There are also numerous OIB localities where 'intermediate ^{3}He/^{4}He' (>10 but <20 R_A) occurs, such as Réunion (e.g., Graham et al., 1990; Staudacher et al., 1990; Hanyu et al., 2001; Trieloff et al., 2002; Hopp and Trieloff, 2005; Füri et al., 2010), and others where the maximum measured ^{3}He/^{4}He ratios are the same or lower than MORB; Canary Island lavas fall within this category. While OIB are characterized in some studies by their highest ^{3}He/^{4}He, it should be recognized that helium isotopic compositions within and between islands can be variable. Heterogeneity in helium isotopes is evident in the Canary Islands, Iceland, the Azores and Hawaii based on comparisons of geothermal fluids and gases and mineral and glass measurements (Day and Hilton, 2021). Examples of significant He isotope heterogeneity from mineral and glass samples also exist in nearly every other OIB location, including notable examples for Samoa (Poreda and Farley, 1992; Jackson et al., 2009), the Azores (Madureira et al., 2005; Moreira et al., 2012) and the Galapagos (Kurz et al., 2009).

To date, at least ten OIB localities have sufficient Ne isotope data to provide 'endmember' extrapolated ^{21}Ne/^{22}Ne ratios to compare with radiogenic isotope systematics (Sr-Nd-Os-Pb) (Fig. 7; Table S2). Extrapolation of the ^{21}Ne/^{22}Ne ratio is done to a ^{20}Ne/^{22}Ne ratio considered to reflect a primordial value. The choice of ^{20}Ne/^{22}Ne with which to extrapolate to relies on knowledge of likely mantle components inherited during terrestrial accretion, with Solar Wind (~13.8), a solar nebula component (~13.4) and a solar irradiation component, sometime referred to as Ne-B (12.5) all representing possible end-member compositions (e.g., Black, 1972; Honda et al., 1993; Trieloff et al., 2000; Moreira, 2013; Péron et al., 2017; Marty, 2020). For the single Canary sample with non-air like Ne (LZ0605), and other OIB, extrapolation was performed to the lower value of 12.5, consistent with calculations for MORB (e.g., Sarda et al., 1988). Extrapolation is done by calculating the extrapolated ^{21}Ne/^{22}Ne ratio as:

$$^{21}\mathrm{Ne}/^{22}\mathrm{Ne}_{\mathrm{ext}} = (((^{21}\mathrm{Ne}/^{22}\mathrm{Ne}_{\mathrm{Measured}} - 0.029)/((^{20}\mathrm{Ne}/^{22}\mathrm{Ne}_{\mathrm{Measured}} - 9.8)/(12.5\text{–}9.8) + 0.029)).$$

where 12.5 is the extrapolated 'solar irradiation' ^{20}Ne/^{22}Ne ratio, and 0.029 and 9.8 are the atmospheric ratios for ^{21}Ne/^{22}Ne and ^{20}Ne/^{22}Ne, respectively (Moreira and Allègre, 1998).

As noted above, the Lanzarote harzburgite may provide evidence for a refractory mantle (RM) source composition. Such a source might be anticipated to play a more pronounced role for OIB close to ridges or in hotspots where high degrees of partial melting take place to enable melting of such a reservoir. This might include parts of Iceland, the western Azores (Terceira) (Madureira et al., 2005; Waters et al., 2020), or rejuvenated lavas such as those on Savaii (Poreda and Farley, 1992; Jackson et al., 2009). The concept of a refractory mantle (RM) component is not new; numerous studies have proposed such an endmember in OIB sources (e.g., Frey et al., 2005; Shorttle et al., 2014; Buchs et al., 2016; Stracke et al., 2019; Harrison et al., 2020; Nicklas et al., 2021). To date, noble gas isotopic evidence in support of such a source within OIB has been sparse. This may be due to the inherent difficulty of recognizing nucleogenic Ne within mantle sources otherwise dominated by less degassed components, much in a similar way to long-lived radiogenic components.

Illustrative models are presented to consider possible mixing relationships between OIB mantle reservoirs with primitive Ne components and high-^{3}He/^{4}He and with HIMU or EM compositions with MORB (DMM) or RM reservoirs in Fig. 7. Models are illustrative since the noble gas contents of the reservoirs are unconstrained, but the ^{3}He/^{22}Ne ratios have been more readily determined (Moreira and Allègre, 1998; Moreira et al., 1998, 2001;

Hopp and Trieloff, 2008; Tucker et al., 2012). Workers have shown that degassing events in the Earth have led to different $^3He/^{22}Ne$ ratios between DMM (~10) and primitive reservoirs (~2.3–3) compared with the solar value (1.5; Tucker et al., 2012). Hyperbolic mixing trends between MORB/RM and a solar component (Fig. 7a) are shown at r = 3 and r = 10 and support prior work suggesting a purely primordial endmember no longer exists, due to radiogenic/nucleogenic ingrowth (e.g., Hopp and Trieloff, 2008). The models assume that FOZO-type lavas have the greatest contribution from a primitive component and it has previously been suggested that the most gas-rich mantle components involved in the formation of OIB dominate the noble gas budget (Hanyu and Kaneoka, 1997; Day and Hilton, 2011). The models for Ne-He mixing support this suggestion but may also imply wider separation of noble gas isotope systematics from lithophile radiogenic isotope signatures.

Previously, high-$^3He/^4He$ OIB locations (>25R_A) have been shown to have similar He, Ne, Sr, Nd and Pb isotope compositions and have been interpreted to reflect contributions from the 'FOZO' reservoir. Whether this source is a mixture of recycled materials and primordial components or is a relatively pristine mantle component is still debated (e.g., Hart et al., 1992; Day et al., 2010; Jackson et al., 2020). In contrast, OIB with HIMU-type and EM signatures can be distinguished from these samples by lower $^3He/^4He$ and generally higher extrapolated $^{21}Ne/^{22}Ne$ (Fig. 7a). Ocean island basalts with FOZO or EM signatures extrapolate from broadly solar Ne and He to MORB-like compositions, indicating some degree of coupling between these systems. HIMU-type lavas, on the other hand, seem to follow distinct trajectories in terms of He-Ne isotope systematics.

When Ne isotopes are compared with radiogenic isotope systematics a remarkable aspect is the overlap between HIMU and FOZO for Nd (and Sr; not shown) and for the EM components for Os (Fig. 7b, c). These He-Sr-Nd-Pb-Os isotope compositions can be explained if HIMU lavas come from sources with similar time-integrated Rb/Sr and Sm/Nd, but higher U/Pb and Re/Os and $(U + Th)/^3He$ than FOZO mantle. On the other hand, EM lavas can be explained if they come from sources with distinctly higher Rb/Sr, $(U + Th)/^3He$ and higher Sm/Nd, but with mantle-like Re/Os. These results provide ambiguity as to whether FOZO could represent a primitive reservoir free from later contamination by recycled materials or is a mixture of primitive and recycled materials. Critical to this comparison, nearly all OIB emanate from mantle sources with indications of a primordial Ne component compared with MORB. Even locations which may have a strong MORB or refractory mantle component (e.g., Terceira) can contain this component. A conclusion that can be made

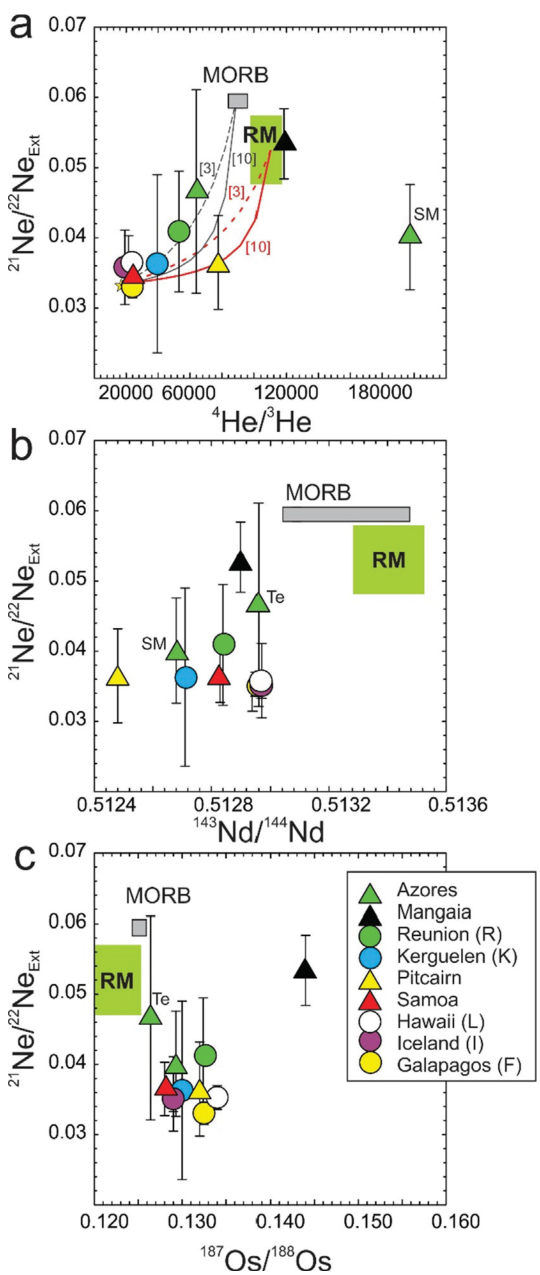

Fig. 7. Extrapolated $^{21}Ne/^{22}Ne$ (to solar irradiation $^{20}Ne/^{22}Ne$ composition of 12.5) versus (a) $^4He/^3He$, (b) $^{143}Nd/^{144}Nd$ and (c) $^{187}Os/^{188}Os$ for a range of OIB and Iceland. Data and sources are given in Table S2. Islands are shown as symbols (Te = Terceira and SM = São Miguel, Azores), and isotopic variations within some island groups are likely to be larger than shown. For example, the value for Samoa is for an extreme He isotopic Ofu sample, whereas rocks from Savaii have higher $^4He/^3He$ and lower $^{143}Nd/^{144}Nd$ (e.g., Poreda and Farley, 1992). Iceland, Hawaii (Loihi = L), Galapagos (Fernandina = F), and Samoa (O = Ofu) define a FOZO component. Model in panel A shows models between a MORB component or a potential refractory mantle component (RM) defined by LZ0605, with a solar Ne component ($^{21}Ne/^{22}Ne_{ext}$ = ~0.033; $^4He/^3He$ = 18,000; shown as a small star). The hyperbolic correlation with curve parameter r = 10 shown, modified from Hopp and Treiloff (2008), where r is the relation of $(^3He/^{22}Ne_{MORB})/(^3He/^{22}Ne_P)$, where P is the primordial mantle component corrected for early degassing events. The $^3He/^{22}Ne_{MORB}$ = ~10 and $^3He/^{22}Ne_P$ is estimated at 2.3–3 (r = ~3), compared to $^3He/^{22}Ne_{Solar}$ of 1.5 (Tucker et al., 2012).

from these types of diagram (Fig. 7) is that all OIB may have distinct He isotope compositions, but must all contain a mantle source component that is less degassed than the MORB source mantle. Consequently, FOZO OIB are not the only materials directly sourced from the deep mantle such that refractory element radiogenic isotope signatures interpreted to be from such sources may not be unique to FOZO.

5. CONCLUSIONS

Helium-Ne-Ar isotope data for Canary Island lavas and cumulate and mantle xenoliths from Lanzarote, El Hierro and La Palma indicate a range in olivine He isotope compositions across the archipelago from 6.9 to 9.7R_A, consistent with He isotope variations in space and time. These samples can have $^{40}Ar/^{36}Ar$ greater than air but have neon isotope compositions that fall within the values for air. New He-Ne-Ar isotope systematics are also reported for mantle peridotite xenoliths interpreted to be refractory harzburgites after partial melting. The peridotites are characterized by having $^{3}He/^{4}He$ (6.6R_A) lower than MORB and nucleogenic $^{21}Ne/^{22}Ne$ at or below the MORB composition and similar to continental lithospheric mantle. These samples may be characteristic of refractory mantle domains that are more depleted than the depleted MORB mantle. Inclusion of refractory mantle (RM) domains as a potential sixth component in OIB, as well as in partial melt sources from convergent and divergent margin settings, could potentially aid in explaining the highly variable He-Ne-Ar isotope systematics observed in some mantle-derived melts.

DECLARATION OF COMPETING INTEREST

The author declares no known competing financial interests or personal relationships that could have appeared to influence the work reported in this paper.

ACKNOWLEDGEMENTS

This paper is dedicated to the memory of David R. Hilton (1958-2018) who tragically passed away before this work could be completed. Doshik Hahm is gratefully acknowledged for assistance with data generation. Jens Hopp, seven anonymous reviewers and the Associate Editor Manuel Moreira are all thanked for their helpful, constructive comments. The research was supported by the NSF Petrology and Geochemistry program (NSF EAR 1447130 and EAR 1918322 to JMDD, and EAR 0439122 to David Hilton).

APPENDIX A. SUPPLEMENTARY MATERIAL

Supplementary data to this article can be found online at https://doi.org/10.1016/j.gca.2022.06.002.

REFERENCES

Allègre C. J., Staudacher T., Sarda P. and Kurz M. (1983) Constraints on evolution of Earth's mantle from rare gas systematics. *Nature* **303**, 762–766.

Amsellem E., Moynier F., Bertrand H., Bouyon A., Mata J., Tappe S. and Day J. M. D. (2020) Calcium isotopic evidence for the mantle sources of carbonatites. *Sci. Adv.* **6**, eaba3269.

Benkert J. P., Baur H., Signer P. and Wieler R. (1993) He, Ne, and Ar from the solar wind and solar energetic particles in lunar ilmenites and pyroxenes. *J. Geophys. Res.* **98**, 13147–13162.

Bianco T. A., Ito G., Becker J. M. and Garcia M. O. (2005) Secondary Hawaiian volcanism formed by flexural arch decompression. *Geochem. Geophys. Geosyst.* **6**(8).

Black D. C. (1972) On the origins of trapped helium, neon and argon isotopic variations in meteorites—II. Carbonaceous meteorites. *Geochim. Cosmochim. Acta* **36**, 377–394.

Buchs D. M., Hoernle K., Hauff F. and Baumgartner P. O. (2016) Evidence from accreted seamounts for a depleted component in the early Galapagos plume. *Geology* **44**, 383–386.

Buikin A., Trieloff M., Hopp J., Althaus T., Korochantseva E., Schwarz W. H. and Altherr R. (2005) Noble gas isotopes suggest deep mantle plume source of late Cenozoic mafic alkaline volcanism in Europe. *Earth Planet. Sci. Lett.* **230**, 143–162.

Burnard P. G., Farley K. A. and Turner G. (1998) Multiple fluid pulses in a Samoan harzburgite. *Chem. Geol.* **147**, 99–114.

Carnevale G., Caracausi A., Correale A., Italiano L. and Rotolo S. G. (2021) An Overview of the Geochemical Characteristics of Oceanic Carbonatites: New Insights from Fuerteventura Carbonatites (Canary Islands). *Minerals* **11**, 203.

Carracedo J. C. and Troll V. R. (2016) *The Geology of the Canary Islands*. Elsevier, p. 636.

Craig H., Marti K. and Wiens R. (1993) *A static mass spectrometer with triple collection for nitrogen and neon isotopes* Tech. Rep. 93-11. Scripps Inst. Oceanogr., San Diego, p. 37.

Day J. M. D. (2013) Hotspot volcanism and highly siderophile elements. *Chem. Geol.* **341**, 50–74.

Day J. M. D. and Hilton D. R. (2011) Origin of $^{3}He/^{4}He$ ratios in HIMU-type basalts constrained from Canary Island lavas. *Earth Planet. Sci. Lett.* **305**, 226–234.

Day J. M. D. and Hilton D. R. (2021) Heterogeneous mantle-derived $^{3}He/^{4}He$ in the Canary Islands and other ocean islands. *Geology* **49**, 120–124.

Day J. M. D., Pearson D. G., Macpherson C. G., Lowry D. and Carracedo J.-C. (2009) Pyroxenite-rich mantle formed by recycled oceanic lithosphere: oxygen-osmium isotope evidence from Canary Island lavas. *Geology* **37**, 555–558.

Day J. M. D., Pearson D. G., Macpherson C. G., Lowry D. and Carracedo J.-C. (2010) Evidence for distinct proportions of subducted oceanic crust and lithosphere in HIMU-type mantle beneath El Hierro and La Palma, Canary Islands. *Geochim. Cosmochim. Acta* **74**, 6565–6589.

Day J. M. D., Barry P. H., Hilton D. R., Pearson D. G., Burgess R. and Taylor L. A. (2015) The helium flux from the continents and ubiquity of low-$^{3}He/^{4}He$ recycled crust and lithosphere. *Geochim. Cosmochim. Acta* **153**, 116–133.

Day J. M. D., Walker R. J. and Warren J. M. (2017) ^{186}Os-^{187}Os and highly siderophile element abundance systematics of the mantle revealed by abyssal peridotites and Os-rich alloys. *Geochim. Cosmochim. Acta* **200**, 232–254.

Day J. M. D., Harvey R. P. and Hilton D. R. (2019) Melt-modified lithosphere beneath Ross Island and its role in the tectono-magmatic evolution of the West Antarctic Rift System. *Chem. Geol.* **518**, 45–54.

Day J. M. D., Jones T. D. and Nicklas R. W. (2022) Mantle sources of ocean islands basalts revealed from noble gas isotope systematics. *Chem. Geol.* **587**, 120626.

Doucet S., Moreira M., Weis D., Scoates J. S., Giret A. and Allegre C. (2006) Primitive neon and helium isotopic compositions of high-MgO basalts from the Kerguelen Archipelago, Indian Ocean. *Earth Planet. Sci. Lett.* **241**, 65–79.

Farley K. A. and Neroda E. (1998) Noble gases in the Earth's mantle. *Annu. Rev. Earth Planet. Sci.* **26**, 189–218.

Frey F. A., Huang S., Blichert-Toft J., Regelous M. and Boyet M. (2005) Origin of depleted components in basalt related to the Hawaiian hot spot: Evidence from isotopic and incompatible element ratios. *Geochem. Geophys. Geosyst.* **6**(2).

Füri E., Hilton D. R., Halldórsson S. A., Barry P. H., Hahm D., Fischer T. P. and Grönvold K. (2010) Apparent decoupling of the He and Ne isotope systematics of the Icelandic mantle: The role of He depletion, melt mixing, degassing fractionation and air interaction. *Geochim. Cosmochim. Acta* **74**, 11.

Gautheron C., Moreira M. and Allègre C. (2005) He, Ne and Ar composition of the European lithospheric mantle. *Chem. Geol.* **217**, 97–112.

Graham D. W. (2002) Noble gases in MORB and OIB: observational constraints for the characterization of mantle source reservoirs. *Rev. Mineral. Geochem.* **46**, 247–318.

Graham D. W., Lupton F., Albarède F. and Condomines M. (1990) Extreme temporal homogeneity of helium isotopes at Piton de la Fournaise, Réunion. *Nature* **347**, 545–548.

Grachev A. F. (2012) MORB-like mantle beneath Lanzarote Island, Canary Islands. *Russ. J. Earth Sci.* **12**, ES3004.

Gurenko A. A., Hoernle K. A., Hauff F., Schmincke H.-U., Han D., Miura Y. N. and Kaneoka I. (2006) Major, trace element and Nd–Sr–Pb–O–He–Ar isotope signatures of shield stage lavas from the central and western Canary Islands: insights into mantle and crustal processes. *Chem. Geol.* **233**, 75–112.

Hanyu T. and Kaneoka I. (1997) The uniform and low $^{3}He/^{4}He$ ratios of HIMU basalts as evidence for their origin as recycled materials. *Nature* **390**, 273–276.

Hanyu T., Clague D. A., Kaneoka I., Dunai T. J. and Davies G. R. (2005) Noble gas systematics of submarine alkalic lavas near the Hawaiian hotspot. *Chemical Geology* **214**(1–2), 135–155.

Hanyu T., Dunai T. J., Davies G. R., Kaneoka I., Nohda S. and Uto K. (2001) Noble gas study of the Reunion hotspot: evidence for distinct less-degassed mantle sources. *Earth Planet. Sci. Lett.* **193**, 83–98.

Hanyu T., Tatsumi Y. and Kimura J. I. (2011) Constraints on the origin of the HIMU reservoir from He–Ne–Ar isotope systematics. *Earth Planet. Sci. Lett.* **307**, 377–386.

Harrison L. N., Weis D. and Garcia M. O. (2020) The multiple depleted mantle components in the Hawaiian-Emperor chain. *Chem. Geol.* **532**, 119324.

Hart S. R., Hauri E. H., Oschmann L. A. and Whitehead J. A. (1992) Mantle plumes and entrainment: isotopic evidence. *Science* **256**, 517–520.

Hilton D. R., Hammerschmidt K., Teufel S. and Freidrichsen H. (1993) Helium isotope characteristics of Andean geothermal fluids and lavas. *Earth Planet. Sci. Lett.* **120**, 265–282.

Hilton D. R., Grönvold K., Macpherson C. G. and Castillo P. R. (1999) Extreme $^{3}He/^{4}He$ ratios in northwest Iceland: constraining the common component in mantle plumes. *Earth Planet. Sci. Lett.* **173**, 53–60.

Hilton D. R., Macpherson C. G. and Elliott T. R. (2000) Helium isotope ratios in mafic phenocrysts and geothermal fluids from La Palma, the Canary Islands (Spain): Implications for HIMU mantle sources. *Geochim. Cosmochim. Acta* **64**, 2119–2132.

Hoernle K., Tilton G. and Schmincke H. U. (1991) Sr-Nd-Pb isotopic evolution of Gran Canaria: Evidence for shallow enriched mantle beneath the Canary Islands. *Earth Planet. Sci. Lett.* **106**, 44–63.

Hofmann A. W. (1997) Mantle geochemistry: the message from oceanic volcanism. *Nature* **385**, 219–229.

Hofmann A. W. and White W. M. (1982) Mantle plumes from ancient oceanic crust. *Earth Planet. Sci. Lett.* **57**, 421–436.

Honda M., McDougall I. and Patterson D. (1993) Solar noble gases in the Earth: the systematics of helium-neon isotopes in mantle derived samples. *Lithos* **30**, 257–265.

Honda M. and Woodhead J. D. (2005) A primordial solar-neon enriched component in the source of EM-I-type ocean island basalts from the Pitcairn Seamounts, Polynesia. *Earth Planet. Sci. Lett.* **236**, 597–612.

Hopp J. and Trieloff M. (2005) Refining the noble gas record of the Réunion mantle plume source: Implications on mantle geochemistry. *Earth Planet. Sci. Lett.* **240**, 573–588.

Hopp J. and Trieloff M. (2008) Helium deficit in high-$^{3}He/^{4}He$ parent magmas: Predegassing fractionation, not a "helium paradox". *Geochem. Geophys. Geosyst.* **9**(3).

Hopp J., Trieloff M. and Altherr R. (2004) Neon isotopes in mantle rocks from the Red Sea region reveal large-scale plume–lithosphere interaction. *Earth Planet. Sci. Lett.* **219**, 61–76.

Hopp J., Trieloff M. and Altherr R. (2007) Noble gas compositions of the lithospheric mantle below the Chyulu Hills volcanic field, Kenya. *Earth Planet. Sci. Lett.* **261**, 635–648.

Jackson M. G., Kurz M. D. and Hart S. R. (2009) Helium and neon isotopes in phenocrysts from Samoan lavas: Evidence for heterogeneity in the terrestrial high $^{3}He/^{4}He$ mantle. *Earth Planet. Sci. Lett.* **287**, 519–528.

Jackson M. G., Blichert-Toft J., Halldórsson S. A., Mundl-Petermeier A., Bizimis M., Kurz M. D., Price A. A., Harðardóttir S., Willhite L. N., Breddam K. and Becker T. W. (2020) Ancient helium and tungsten isotopic signatures preserved in mantle domains least modified by crustal recycling. *Proc. Natl. Acad. Sci.* **117**, 30993–31001.

Kaneoka I. (1983) Noble gas constraints on the layered structure of the mantle. *Nature* **302**, 698–700.

Klügel A., Galipp K., Hoernle K., Hauff F. and Groom S. (2017) Geochemical and volcanological evolution of La Palma, Canary Islands. *J. Petrol.* **58**, 1227–1248.

Kurz M. D., Jenkins W. J. and Hart S. R. (1982) Helium isotopic systematics of oceanic islands and mantle heterogeneity. *Nature* **297**, 43–47.

Kurz M. D., Curtice J., Fornari D., Geist D. and Moreira M. (2009) Primitive neon from the center of the Galápagos hotspot. *Earth Planet. Sci. Lett.* **286**, 23–34.

Madureira P., Moreira M., Mata J. and Allègre C. J. (2005) Primitive neon isotopes in Terceira Island (Azores archipelago). *Earth Planet. Sci. Lett.* **233**, 429–440.

Marty B. (2020) Origins and early evolution of the atmosphere and oceans. *Geochem. Perspect.* **9**, 1–313.

Mata J., Moreira M., Doucelance R., Ader M. and Silva L. C. (2010) Noble gas and carbon isotopic signatures of Cape Verde oceanic carbonatites: implications for carbon provenance. *Earth Planet. Sci. Lett.* **291**, 70–83.

Moreira M. (2013) Noble gas constraints in the origin and evolution of Earth's volatiles. *Geochem. Perspect.* **2**, 1–403.

Moreira M. and Allègre C. J. (1998) Helium–neon systematics and the structure of the mantle. *Chem. Geol.* **147**, 53–59.

Moreira M. and Kurz M. D. (2001) Subducted oceanic lithosphere and the origin of the 'high μ' basalt helium isotopic signature. *Earth Planet. Sci. Lett.* **189**, 49–57.

Moreira M., Kunz J. and Allegre C. (1998) Rare gas systematics in popping rock: isotopic and elemental compositions in the upper mantle. *Science* **279**, 1178–1181.

Moreira M., Breddam K., Curtice J. and Kurz M. D. (2001) Solar neon in the Icelandic mantle: new evidence for an undegassed lower mantle. *Earth Planet. Sci. Lett.* **185**, 15–23.

Moreira M., Kanzari A. and Madureira P. (2012) Helium and neon isotopes in São Miguel island basalts, Azores Archipelago: new constraints on the "low ^{3}He" hotspot origin. *Chem. Geol.* **322–323**, 91–98.

Mukhopadhyay S. (2012) Early differentiation and volatile accretion recorded in deep-mantle neon and xenon. *Nature* **486**, 101–104.

Niedermann S., Graf T. and Marti K. (1993) Mass spectrometric identification of cosmic-ray produced neon in terrestrial rocks with multiple neon components. *Earth Planet. Sci. Lett.* **118**, 65–73.

Nicklas R. W., Brandon A. D., Waight T. E., Puchtel I. S. and Day J. M. D. (2021) High-precision Pb and Hf isotope and highly siderophile element abundance systematics of high-MgO Icelandic lavas. *Chem. Geol.* **582**, 120436.

Parai R., Mukhopadhyay S. and Lassiter J. C. (2009) New constraints on the HIMU mantle from neon and helium isotopic compositions of basalts from the Cook-Austral Islands. *Earth Planet. Sci. Lett.* **277**, 253–261.

Parai R., Mukhopadhyay S. and Standish J. J. (2012) Heterogeneous upper mantle Ne, Ar and Xe isotopic compositions and a possible Dupal noble gas signature recorded in basalts from the Southwest Indian Ridge. *Earth Planet. Sci. Lett.*, 227–239.

Paquet M., Day J. M. D. and Castillo P. (2019) Osmium isotope evidence for a heterogeneous ^{3}He/^{4}He mantle plume beneath the Juan Fernandez Islands. *Geochim. Cosmochim. Acta* **261**, 1–19.

Perez N. M., Wakita H., Nakai S., Sano Y. and Williams S. N. (1994) ^{3}He/^{4}He isotopic ratios in volcanic-hydrothermal discharges from the Canary Islands, Spain: implications on the origin of the volcanic activity. *Mineral. Mag.* **58A**, 709–710.

Péron S., Moreira M., Putlitz B. and Kurz M. D. (2017) Solar wind implantation supplied light volatiles during the first stage of Earth accretion. *Geochem. Perspect. Lett.* **3**, 151–159.

Poreda R. J. and Farley K. A. (1992) Rare gases in Samoan xenoliths. *Earth Planet. Sci. Lett.* **113**, 129–144.

Sarda P., Staudacher T. and Allegre C. J. (1988) Neon isotopes in submarine basalts. *Earth Planet. Sci. Lett.* **91**, 73–88.

Shaw A. M., Hilton D. R., Macpherson C. G. and Sinton J. M. (2001) Nucleogenic neon in high ^{3}He/^{4}He lavas from the Manus back-arc basin: a new perspective on He–Ne decoupling. *Earth Planet. Sci. Lett.* **194**, 53–66.

Shorttle O., Maclennan J. and Lambart S. (2014) Quantifying lithological variability in the mantle. *Earth Planet. Sci. Lett.* **395**, 24–40.

Snortum E., Day J. M. D. and Jackson M. G. (2019) Pacific mantle lithosphere evolution inferred from Aitutaki mantle xenoliths. *J. Petrol.* **60**, 1753–1772.

Stracke A., Snow J. E., Hellebrand E., Von Der Handt A., Bourdon B., Birbaum K. and Günther D. (2011) Abyssal peridotite Hf isotopes identify extreme mantle depletion. *Earth Planet. Sci. Lett.* **308**, 359–368.

Stracke A., Genske F., Berndt J. and Koornneef J. M. (2019) Ubiquitous ultra-depleted domains in Earth's mantle. *Nat. Geosci.* **12**, 851–855.

Staudacher T., Sarda P. and Allègre C. J. (1990) Noble gas systematics of Réunion island, Indian Ocean. *Chem. Geol.* **89**, 1–17.

Simon N. S. C., Neumann E.-R., Bonadiman C., Coltorti M., Delpech G., Grégoire M. and Widom E. (2008) Ultra-refractory domains in the oceanic lithosphere sampled as mantle xenoliths in ocean islands. *J. Petrol.* **49**, 1223–1251.

Trieloff M., Kunz J., Clague D. A., Harrison D. and Allègre C. J. (2000) The nature of pristine noble gases in mantle plume. *Science* **288**, 1036–1038.

Trieloff M., Kunz J. and Allègre C. J. (2002) Noble gas systematics of the Réunion mantle plume source and the origin of primordial noble gases in Earth's mantle. *Earth Planet. Sci. Lett.* **200**, 297–313.

Tucker J. M., Mukhopadhyay S. and Schilling J. G. (2012) The heavy noble gas composition of the depleted MORB mantle (DMM) and its implications for the preservation of heterogeneities in the mantle. *Earth Planet. Sci. Lett.* **355**, 244–254.

Valbracht P. J., Staudacher T., Malahoff A. and Allegre C. J. (1997) Noble gas systematics of deep rift zone glasses from Loihi Seamount, Hawaii. *Earth Planet. Sci. Lett.* **150**, 399–411.

Valbracht P. J., Honda M., Matsumoto T., Mattielli N., McDougall I., Ragettli R. and Weis D. (1996) Helium, neon and argon isotope systematics in Kerguelen ultramafic xenoliths: implications for mantle source signatures. *Earth Planet. Sci. Lett.* **138**, 29–38.

Vance D., Stone J. O. H. and O'Nions R. K. (1989) He, Sr and Nd isotopes in xenoliths from Hawaii and other oceanic islands. *Earth Planet. Sci. Lett.* **96**, 147–160.

Waters C. L., Day J. M. D., Watanabe S., Hanan B. B., Zayit A., Olson K., Zanon V. and Widom E. (2020) Sulfide mantle source heterogeneity recorded in Azorean lavas. *Geochim. Cosmochim. Acta* **268**, 422–445.

Wetherill G. W. (1954) Variations in the isotopic abundances of neon and argon extracted from radioactive minerals. *Physical Reviews* **96**(3), 679–683.

Widom E., Hoernle K. A., Shirey S. B. and Schmincke H.-U. (1999) Os isotope systematics in the Canary Islands and Madiera: lithospheric contamination and mantle plume signatures. *J. Petrol.* **40**, 279–296.

Yatsevich I. and Honda M. (1997) Production of nucleogenic neon in the Earth from natural radioactive decay. *J. Geophys.* **102**, 10291–10298.

Zindler A. and Hart S. R. (1986) Chemical geodynamics. *Annu. Rev. Earth Planet. Sci.* **14**, 493–571.

Associate editor: Manuel Moreira